IEEE Photonics Journal
An IEEE Photonics Society Publication

Open Access

Remote Low-Coherence Fiber Vibrometer With Wide Dynamic Range

Volume 7, Number 3, June 2015

Hui Li
Jian Chen
Xiaoguang Wang
Shenglai Zhen
Benli Yu

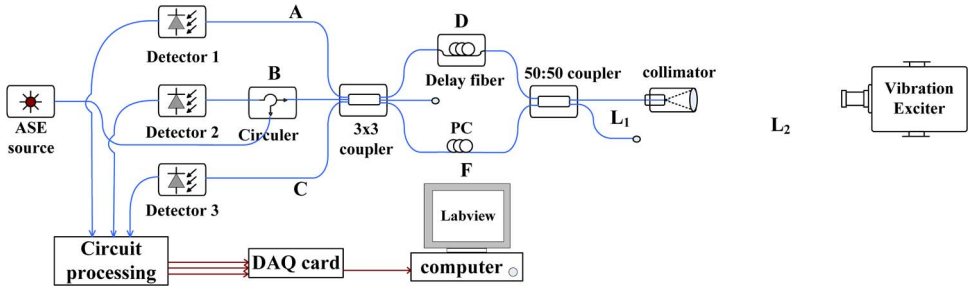

DOI: 10.1109/JPHOT.2015.2425302
1943-0655 © 2015 IEEE

IEEE photonics SOCIETY

IEEE

Remote Low-Coherence Fiber Vibrometer With Wide Dynamic Range

Hui Li, Jian Chen, Xiaoguang Wang, Shenglai Zhen, and Benli Yu

Key Laboratory of Opto-Electronic Information Acquisition and Manipulation of Ministry of Education, Anhui University, Hefei 230601, China

DOI: 10.1109/JPHOT.2015.2425302

Manuscript received March 24, 2015; revised April 15, 2015; accepted April 17, 2015. Date of publication April 22, 2015; date of current version May 6, 2015. This work was supported in part by the Natural Science Foundation of Anhui Province under Grant 1308085MF91 and in part by the Key Science and Technology Program of Anhui Province under Grant 1310115197. Corresponding author: S. Zhen (e-mail: slzhen@ahu.edu.cn).

Abstract: We present a remote low-coherence fiber vibrometer, which is composed of a hybrid configuration of Mach–Zehnder and Sagnac interferometer. In the interferometer, the signal and reference beams travel along the same path but in opposite directions. Owing to the fiber differential interferometric theory and a passive demodulation algorithm, absolute amplitude at a distance more than 1 m could be measured. The experimental results demonstrate that the vibrometer has a wide dynamic range for amplitude measurement from 4.34 pm to 2.43 mm. The deviation of measured amplitude is less than 0.8 dB, and the frequency response range is 30 Hz–11 kHz. The proposed method is potentially suitable for applications that require noncontact and high-dynamic-range measurements.

Index Terms: Low coherence, remote, vibrometer.

1. Introduction

Vibration monitoring has played an increasing role in important machines, such as power station turbines and generators, to give an early warning of risky conditions in machines [1]. A large number of methods have been proposed to measure the frequency and amplitude of vibration by mechanical, electrical, and optical devices [2], [3]. The high-performance non-contact sensors constructed by optical fibers have already been established, due to their excellent physical advantages, such as high sensitivity, large resistance to electromagnetic interference, and low transmission loss [3], [4].

Generally, fiber optic vibration sensors are divided into two types according to their working principle: phase and intensity modulation. The phase-modulated fiber optic sensors using Michelson [5], Mach–Zehnder [6], Sagnac [7], or Self-mixing [8] interferometric techniques have a history of long utilization due to their higher sensitivity and accuracy, as well as larger dynamic range than intensity-modulated sensors [1]. Those sensors can be used to measure a variety of parameters such as absolute distance, speed [9], vibration [10], and temperature [11]. Conventional high-coherence fiber interferometers have the quadrature point fading problem caused by external perturbations. Jackson and Jones proposed several active and passive compensating schemes to overcome this problem [12]. Low-coherence or white light interferometry was used to measure the vibration amplitude absolutely for over one wavelength of vibration.

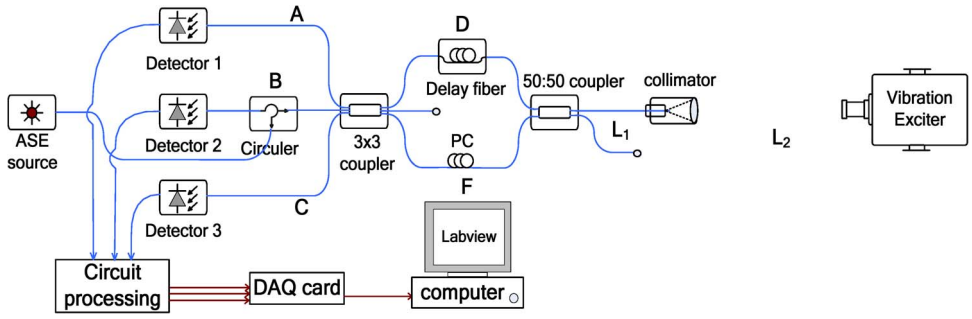

Fig. 1. Experimental setup.

This technique was first reported in fiber optic sensing by Al Chalabi *et al.* Weir measured the vibration using low-coherence Michelson interferometer, which includes two parts: sensing interferometer and receive interferometer [13]. A hybrid interferometer structure was set up and implemented the pipeline leak detection and location by Shih-Chu Huang *et al.* in 2007 [14]. Ambali Taiwo proposed a method to implement vibration sensor multiplexing which can eliminate the Multiple Access Interference at low cost and complexity in 2014 [15]. Fang presented a low coherence fiber differentiating interferometer and its passive demodulation schemes, which extended the vibration measurement range [16].

In general, these methods of measuring vibration by fiber optic low-coherence interferometer require physical contact with the vibrating object, or In line with the optical path difference matching conditions through mechanical adjustment. In this paper, a low coherence fiber differential interferometer with wide dynamic range for absolute amplitude measurement is proposed. It is a hybrid configuration composed of Mach–Zehnder and Sagnac without mechanical scanning device. Non-contact absolute amplitude could be measured remotely applying the characteristic of zero optic path difference. The received signal can be demodulated by a passive demodulation scheme [17]. The interferometer can measure frequency and amplitude of vibration. Also, it has great potential in the measurement of velocity and other physical parameters.

2. Experimental Setup and Theoretical Analysis

The setup of fiber differential interferometer is shown in Fig. 1. It is a hybrid configuration of Mach–Zehnder and Sagnac interferometer with three detectors. The interferometer is composed of a low coherence light source, a section of delay fiber, a 2 $\times$ 2 fiber coupler, a 3 $\times$ 3 fiber coupler and a collimator. One terminal of the 3 $\times$ 3 fiber coupler is connected to the light source and a photo detector through a fiber circulator and the other two terminals of the 3 $\times$ 3 fiber coupler are connected to two detectors respectively. Two terminals between 3 $\times$ 3 fiber coupler and 2 $\times$ 2 fiber coupler are directly connected through a polarization controller (PC) and the other two are connected through delay fiber D. In addition, one output terminal of the 2 $\times$ 2 fiber coupler is looped to eliminate the reflected light, another terminal is connected to a collimator, light from the collimator is projected onto a vibration exciter (type: B&K 4809).

In the setup, an amplified spontaneous emission (ASE) light source was adopted as the low coherent source. ASE light source was divided into four paths by a 3 $\times$ 3 fiber coupler and a 2 $\times$ 2 fiber coupler: 1) F $\rightarrow$ L_1 $\rightarrow$ L_2 $\rightarrow$ L_2 $\rightarrow$ L_1 $\rightarrow$ D; 2) D $\rightarrow$ L_1 $\rightarrow$ L_2 $\rightarrow$ L_2 $\rightarrow$ L_1 $\rightarrow$ F; and 3) F $\rightarrow$ L_1 $\rightarrow$ L_2 $\rightarrow$ L_2 $\rightarrow$ L_1 $\rightarrow$ F; 4) D $\rightarrow$ L_1 $\rightarrow$ L_2 $\rightarrow$ L_2 $\rightarrow$ L_1 $\rightarrow$ D. Only paths 1) and 2) have the same optical length and can generate interference signals. Here we know that the phase variation signals produced by a Brüel & Kjær piezoelectric accelerometer are sinusoidal signals, the electric fields of the lights passing through path 1) and path 2) can be expressed as follows [14]:

$$\begin{aligned} \textit{Path } 1: \ E_1 &= E_{10}\exp[j\omega_c t + 2j\Delta\phi\sin\omega(t-\tau_1) + j\psi_1] \\ \textit{Path } 2: \ E_2 &= E_{20}\exp[j\omega_c t + 2j\Delta\phi\sin\omega(t-\tau_2) + j\psi_2] \end{aligned} \quad (1)$$

where E_{10}, E_{20} are the amplitudes of the light beams through Path 1 and Path 2. ω_c is the angular frequency of the optical carrier, $\Delta\phi$ is the peak phase excursion of the desired signal and ω is the signal angular frequency, ψ_1, ψ_2 are the arbitrary optical carrier phase angles. $\tau_1 = n(F + L_1 + L_2)/c$ $\tau_2 = n(D + L_1 + L_2)/c$, are the time duration of passing through vibration position in the Path 1 and Path 2, respectively. c is the speed of light in vacuum, and n is the refractive index of the fiber core.

The total electric field intensity can be represented as

$$\begin{aligned} I &= (E_1 + E_2) \cdot (E_1 + E_2)^* + E_3 \cdot E_3^* + E_4 \cdot E_4^* \\ &= E_1 \cdot E_1^* + E_2 \cdot E_2^* + 2\mathrm{Re}\left(E_1 \cdot E_2^*\right) + E_3 \cdot E_3^* + E_4 \cdot E_4^* \end{aligned} \tag{2}$$

where $2\mathrm{Re}(E_1 \cdot E_2^*)$ is interference item, E_3, E_4 are the electric field intensity of the light path 3 and path 4, (1) and (2) can be expressed as follows:

$$I = E_{10}^2 + E_{20}^2 + 2E_{10}E_{20}\cos\{2\Delta\phi[\sin\omega(t-\tau_1) - \sin\omega(t-\tau_2)] + (\psi_1 - \psi_2)\} + E_{30}^2 + E_{40}^2 \tag{3}$$

where E_{30}, E_{40} are the amplitudes of the light beams through Path 3 and Path 4 respectively, if we ignore the light transmission loss through different paths and the amplitudes of the light beams are all equal, $E_{10} = E_{20} = E_{30} = E_{40} = E_0$ is 1/36 of the amplitude of light source; therefore

$$\begin{aligned} I &= 4E_0^2 + 2E_0^2\cos\{2\Delta\phi[\sin\omega(t-\tau_1) - \sin\omega(t-\tau_2)] + (\psi_1 - \psi_2)\} \\ &= 4E_0^2 + 2E_0^2\cos\left\{4\Delta\phi\cos\omega\left(t - \frac{\tau_1 + \tau_2}{2}\right)\sin\omega\left(\frac{\tau_2 - \tau_1}{2}\right) + (\psi_1 - \psi_2)\right\} \end{aligned} \tag{4}$$

where $\tau_T = \tau_1 + \tau_2 = n(D + F + 2L_1 + 2L_2)/c$ is the time duration of passing through Path 1 or Path 2, and $\tau_d = \tau_2 - \tau_1 = n(D - F)/c$ is the time duration of passing through delay fiber D.

According to the linear symmetric coupler theory, for a 2 $\times$ 2 coupler, the phase at the uncoupled output fiber is $\pi/2$ rad ahead that of its coupled counterpart. The three outputs of the 3 $\times$ 3 coupler are supposed to be completely symmetric, and the coupled output fiber of 3 $\times$ 3 coupler will introduce $2\pi/3$ rad phase shift. After photocurrent to voltage conversion, the three outputs of the PD are given by [17]

$$\begin{aligned} V_1 &= H + E\cos(\varphi - 2\pi/3) \\ V_2 &= H + E\cos\varphi \\ V_3 &= H + E\cos(\varphi + 2\pi/3) \end{aligned} \tag{5}$$

where $\varphi = 4\Delta\phi \cdot \cos\omega(t - (\tau_T/2)) \cdot \sin\omega(\tau_d/2)$ is actual phase difference, H and E are proportional to the light intensity, H is the dc component of the voltage, and E also depends on the visibility of the interference signal.

The received signals from three detectors are circuited and collected by NI data acquisition card PCI-6251. We use the principle of passive homodyne orthogonal demodulation and a symmetrical 3 $\times$ 3 fiber coupler homodyne demodulation. A typical triple detection passive demodulation algorithm is shown in Fig. 2. The unique features of this algorithm, namely an average of three outputs to remove the dc component and the sum of squares to normalize coefficient E^2 of alternating current, are shown explicitly. The core part of actual phase demodulation is the differential and cross-multiplying (DCM). The integration produces an output of the form

$$\int \left[(a+c)' \cdot (a-c) - (a+c) \cdot (a-c)'\right] dt = \sqrt{3}E^2\varphi \tag{6}$$

Therefore, this interferometer is also called differential interferometer. The delay fiber D is much longer than fiber length F, and therefore, $\sin\omega(\tau_d/2) \approx (\omega\tau_d/2)$. After the integral, we can

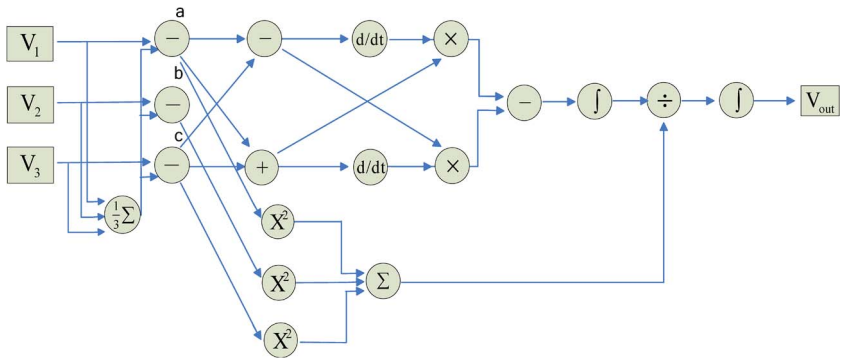

Fig. 2. Schematic diagram of the demodulation method.

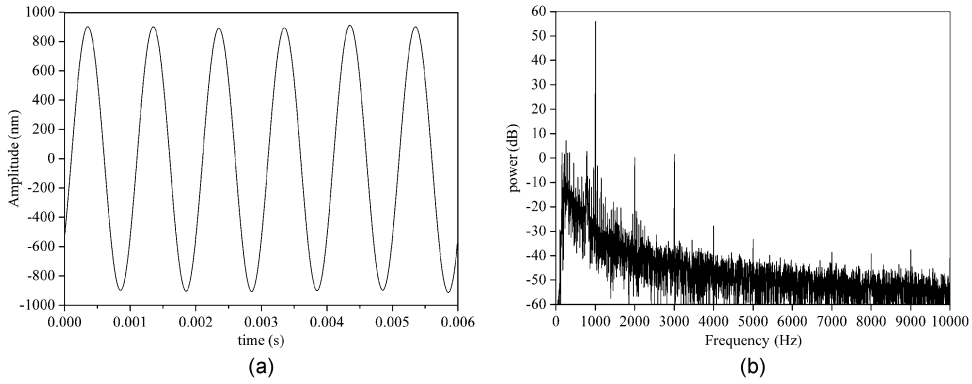

Fig. 3. Oscillograph of demodulation signal (a) time domain and (b) corresponding frequency domain (1 kHz, 921 nm).

get the output V_{out} which contains the amplitude component of signal

$$V_{out} = \frac{2}{\sqrt{3}}\int \varphi dt = \frac{8}{\sqrt{3}\omega}\Delta\phi \cdot \sin\omega\left(\tau - \frac{\tau_T}{2}\right) \cdot \frac{\omega\tau_d}{2} = \frac{4}{\sqrt{3}}\Delta\phi \cdot \tau_d \cdot \sin\omega\left(t - \frac{\tau_T}{2}\right) \tag{7}$$

By counting the amplitude ratio of (7), the amplitude of vibration can be calculated as follows:

$$\Delta\phi = \frac{\sqrt{3}V_{\max}}{4\tau_d} \tag{8}$$

where $\sqrt{3}/4\tau_d$ is the amplitude ratio.

3. Experimental Results and Analysis

The central wavelength of ASE light source is 1550 nm, the length of delay fiber is 2.1 km, and the refractive index of fiber core is 1.4682. The sensing head is based on a fiber collimator. The focal length and numerical aperture of the fiber collimator are 8.18 mm and 0.49 respectively. The interference signals are received by three low-noise p-i-n photodiodes (PIN PD) which are connected to an amplifier circuit, respectively. The circuit outputs are sampled simultaneously using a 16-bit acquisition card with 300 kHz/s sampling rate and then transmitted into a computer to perform the demodulation with LabVIEW.

In order to acquire better measurement results, good and clear interference signal waveform are preferable. The direction and distance from the collimator to oscillator was carefully adjusted

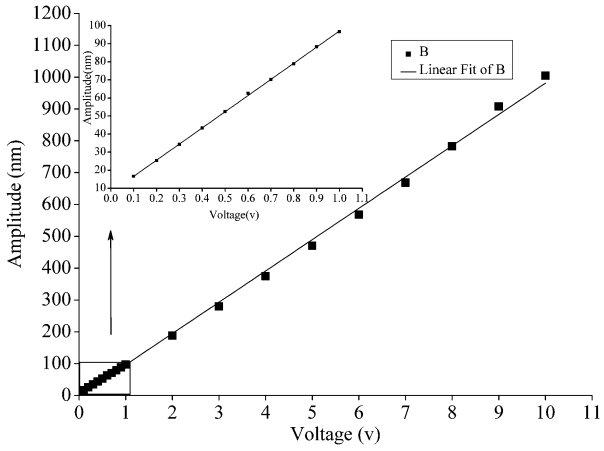

Fig. 4. Correlation of the vibration amplitude and the load voltage from 0.1 v to 10 v at 1 kHz.

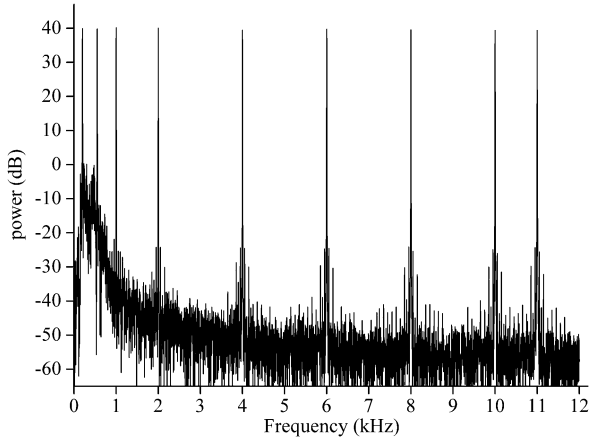

Fig. 5. Stability of amplitude with different frequency ranging from 200 Hz to 11 kHz.

to enhance the optical coupling efficiency for better signals. The Oscillograph of time domain and corresponding frequency domain of vibration are shown in Fig. 3(a) and (b).

Fig. 4 illustrates the relationship between the drive voltage and the corresponding vibration amplitude. When the driving V increased from 0.1 to 10 v at 1 kHz, the corresponding vibration amplitude increased linearly. Fig. 5 depicts the stability of amplitude with frequency ranges from 200 Hz to 11 kHz, the frequency range is restricted by the output capacity of vibration exciter we used in Fig. 5. Those results prove the excellent stability and validity of the measuring results.

To verify the accuracy of the measured vibration amplitudes, we can discuss from two aspects: changing the driving voltage under certain frequency and changing the frequency under certain amplitude, respectively. The results are shown in Figs. 6 and 7 accordingly. In Fig. 6, the maximum amplitude of vibration exciter driven by the function generator can only be 80 dB at 1 kHz. Fig. 7 depicts different measured amplitude with standard amplitude of 40 dB in different frequency ranging from 100 Hz to 10 kHz. Based on these data, the largest deviation was calculated to be less than 0.8 dB.

For researching the dynamic range of the experiment, We need to detect the maximum amplitude and minimum amplitude. Fig. 8 shows that the amplitude of 13 nm calculated from the spectrum diagram at 10 kHz; we can see the signal to noise ratio (SNR) is about 69 dB, and

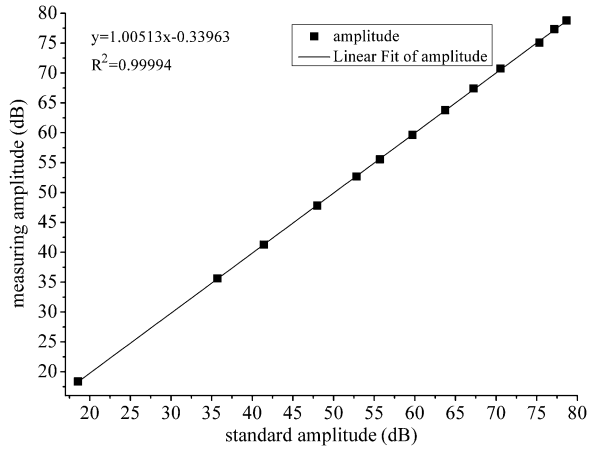

Fig. 6. Correlation of standard and measuring vibration amplitude at 1 kHz.

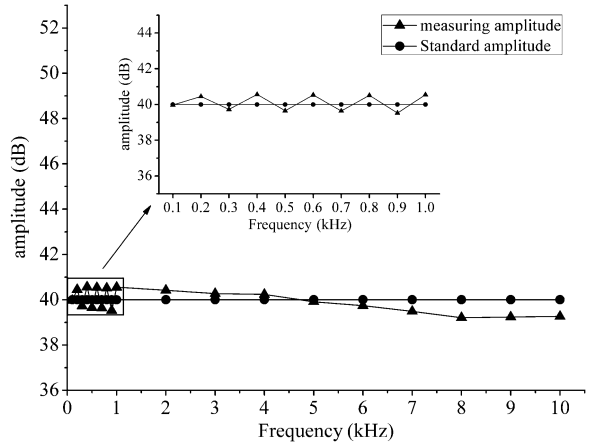

Fig. 7. Correlation of standard and measuring vibration amplitude in different frequency ranging from 100 Hz to 11 kHz.

therefore, we can calculate the amplitude demodulation resolution to be 4.34 pm. Fig. 9 depicts the maximum amplitude of 2.43 mm which is calculated from the spectrum diagram at 30 Hz, because of the amplitude of B&K has an upper limit of 2.8 mm. Combined with practical application, we determine the signal distortion standard: the side-mode suppression ratio (SMSR) is larger than 40 dB. We can see the SMSR is about 50 dB; therefore, the maximum amplitude of the experiment detected does not reach the theoretical limitation and can be enlarged approximately three times. The results show that the detected amplitude range of the experiment is from 4.34 pm to 2.43 mm.

4. Conclusion

In this paper, we first proposed a novel non-contact vibration measurement of low coherent interferometer with more than 1 m measurable distance. The interferometer is based on a hybrid configuration composed of Mach–Zehnder and Sagnac interferometer. The received signal which contains the amplitude component is demodulated by a triple detection passive demodulation scheme. The experimental results show that the vibrometer could measure absolute amplitude of vibration B&K induced. The good linear relationship between the driving voltage and corresponding vibration amplitude, as well as the stability of the measured results, have been

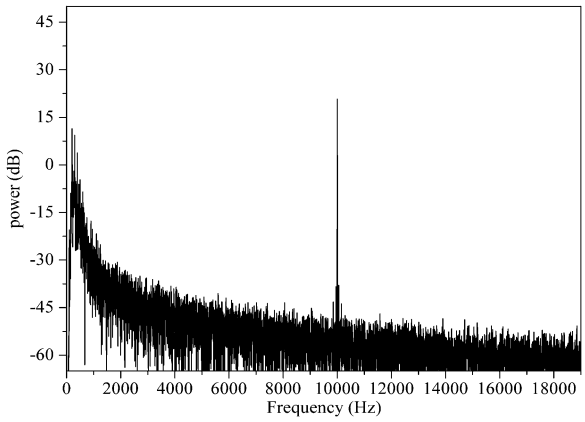

Fig. 8. Spectrum diagram of demodulated amplitude at 10 kHz.

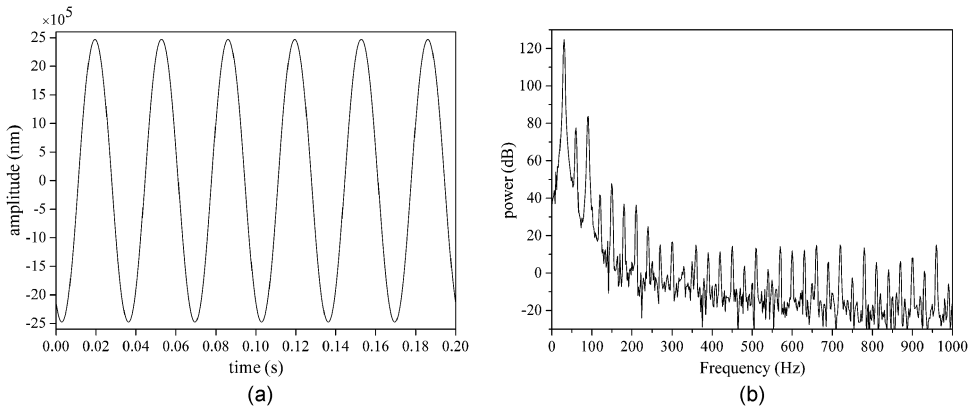

Fig. 9. Oscillograph of (a) time domain and (b) corresponding frequency domain of maximum amplitude at 30 Hz.

proved. The low coherent fiber vibrometer has a wide dynamic measurement range from 4.34 pm to 2.43 mm, which could extended to a large number by increasing the output capacity of vibration exciter. The amplitude demodulated resolution reaches 4.34 pm and the largest deviation is less than 0.8 dB from 4.34 pm to 2.43 mm. In order to achieve higher measurement accuracy and SNR, improving the optic coupling efficiency and broadening the frequency range is quite necessary. Meanwhile, we should reduce the influence of environmental noise and polarization. For the excellent characteristics of vibration measurement, this vibrometer will have great attribute to industrial and medical applications such as pipeline leak, membrane vibration measurement, and so on.

References

[1] P. Kishore, D. Dinakar, K. Srimannarayana, and P. V. Rao, "Vibration sensor using 2 × 2 fiber optic coupler," *Opt. Eng.*, vol. 52, no. 10, Oct. 2013, Art. ID. 107104.
[2] L. Lu, W. H. Zhang, B. Yang, J. X. Zhou, H. Q. Gui, and B. L. Yu, "Dual-channel self-mixing vibration measurement system in a linear cavity fiber laser," *IEEE Sensors J.*, vol. 13, no. 11, pp. 4387–4392, Nov. 2013.
[3] S. Binu, V. P. M. Pillai, and N. Chandrasekaran, "Fibre optic displacement sensor for the measurement of amplitude and frequency of vibration," *Opt. Laser Technol.*, vol. 39, no. 8, pp. 1537–1543, Nov. 2007.
[4] W. Weise, V. Wilkens, and C. Koch, "Frequency response of fiber-optic multilayer hydrophones: Experimental investigation and finite element simulation," *IEEE Trans. Ultrason., Ferroelectr.,Freq. Control*, vol. 49, no. 7, pp. 937–945, Jul. 2002.

[5] T. Li, A. Wang, K. Murphy, and R. Claus, "White-light scanning fiber Michelson interferometer for absolute position—-distance measurement," *Opt. Lett.*, vol. 20, no. 7, pp. 785–787, Apr. 1995.
[6] E. E. Ren, H. W. Lu, B. G. Zhang, and G. W. Luo. "Optimization design of all-fiber 3 × 3 multiplexer based on an asymmetrical Mach-Zehnder interferometer," *Opt. Commun.*, vol. 282, no. 14, pp. 2818–2822, Jul. 2009.
[7] D. F. Wu, T. Z. Zhang, and B. Jia. "Modified Sagnac interferometer for distributed disturbance detection," *Microw. Opt. Technol. Lett.*, vol. 50, no. 6, pp. 1608–1610, Jun. 2008.
[8] Y. H. Zhao, L. Lu, Z. T. Du, B. Yang, W. H. Zhang, J. X. Zhou, H. Q. Gui, and B. L. Yu, "Research on micro-vibration measurement by a laser diode self-mixing interferometer," *Optik—Int. J. Light Electron Opt.*, vol. 124, no. 21, pp. 4707–4711, Nov. 2013.
[9] B. Jia, L. Hu, H. Tan, X. M. Zhou, and K. Z. Ye, "Fiber-optic interferometer for measuring low velocity of diffusely reflecting surface," *Microw. Opt. Technol. Lett.*, vol. 22, no. 4, pp. 231–234, Aug. 1999.
[10] G. Perrone and A. Vallan, "A low-cost optical sensor for noncontact vibration measurements," *IEEE Trans. Instrum. Meas.*, vol. 58, no. 5, pp. 1650–1656, May 2009.
[11] J. H. Kim, "An all fiber white light interferometric absolute temperature measurement system," *Sensors*, vol. 8, no. 11, pp. 6825–6845, 2008.
[12] Y. J. Rao and D. A. Jackson, "Recent progress in fibre optic low-coherence interferometry," *Meas. Sci. Technol.*, vol. 7, no. 7, pp. 981–999, Jul. 1996.
[13] K. Weir, W. J. 0. Boyle, B. T. Meggitt, A. W. Palmer, and K. T. V. Grattan, "A novel adaptation of the Michelson interferometer for the measurement of vibration," *J. Lightw. Technol.*, vol. 10, no. 5, pp. 700–703, May 1992.
[14] S. C. Huang, W. W. Lin, M. T. Tsai, and M. H. Chen, "Fiber optic in-line distributed sensor for detection and localization of the pipeline leaks," *Sensors Actuators A, Phys.*, vol. 135, no. pp. 570–579, Apr. 2007.
[15] A. Taiwo, S. Taiwo, R. K. Z. Sahbudin, M. H. Yaacob, and M. Mokhtar, "Fiber vibration sensor multiplexing techniques for quasi-distributed sensing," *Opt. Laser Technol.*, vol. 64, pp. 34–40, Dec. 2014.
[16] W. T. Fang, Q. M. Jia, S. L. Zhen, J. Chen, X. Y. Cheng, and B. L. Yu, "Low coherence fiber differentiating interferometer and its passive demodulation schemes," *Opt. Fiber Technol.*, vol. 21, pp. 34–39, Jan. 2015.
[17] Z. Q. Zhao, M. S. Demokan, and M. MacAlpine, "Improved demodulation scheme for fiber optic interferometers using an asymmetric 3 × 3 coupler," *J. Lightw. Technol.*, vol. 15, no. 11, pp. 2059–2068, Nov. 1997.